Affine Arithmetic Based Methods for Voltage and Transient Stability Assessment of Power Systems with Intermittent Generation Sources

Juan Muñoz, Claudio Cañizares, Kankar Bhattacharya
ECE Dep., University of Waterloo

Alfredo Vaccaro
Dep. of Engineering, University of Sannio

Abstract

This paper presents novel methods based on Affine Arithmetic (AA) for voltage and transient stability assessment of power systems, considering uncertainties of power injections from intermittent generation sources such as wind and solar. These methods, which are an alternative to the well-known sampling and probabilistic based approaches, are able to improve the computational efficiency as compared to simple Monte Carlo (MC) simulations, with reasonably accuracy. The presented AA-based voltage stability method computes the hull of PV curves associated with the assumed uncertainties, and results are discussed in detail for a 5-bus test system. On the other hand, the proposed AA-based transient stability method solves the set of differential-algebraic equations in affine form, based on a trapezoidal integration approach, that yields the hull of the dynamic response of the system, for a set of assumed contingencies and uncertainties; this approach is demonstrated on a generator-infinite bus test system. In both presented stability studies, MC simulations are used for comparison and validation purposes.

Nomenclature

Indices

c	Index for buses with voltage control settings.
D	Index for dynamic variables, parameters, and functions.
h	Index for approximation noise symbols.
i, k	Bus indices.
IC	Index indicating central values.
j, s	Index associated with differential-algebraic equations.
max	Index for maximum limit.
min	Index for minimum limit.
m	Index for buses with intermittent sources of power.
o	Index indicating initial values.
PF	Index for power flow variables, parameters, and functions.
r	Index indicating iteration number.

Variables

A	Matrix of coefficients for affine forms used in AA-based power flow analysis.
A_{vs}	Matrix of coefficients for affine forms used in AA-based voltage stability assessment (p.u.).
C	Auxiliary vector for linear programming formulation in the AA-based power flow analysis (p.u.).
C_{vs}	Auxiliary vector for the linear programming formulation in the AA-based voltage stability assessment (p.u.).
$\widehat{\Delta F}$	Vector associated with the error of the differential-algebraic equations in affine form.
ΔF_H	Equivalent approximation error of non-affine operations of $\widehat{\Delta F}$.
$\Delta\lambda$	Variation of bifurcation parameter (p.u.).
$\Delta\theta$	Variation of bus voltage angle (p.u.).
$\widehat{\delta}$	Rotor angular position in affine form (rad).
$\widehat{\Delta X}$	Vector of corrections of the state and algebraic variables in affine form.
ΔX_H	Equivalent approximation error introduced by non-affine operations of state and algebraic variables.
$\widehat{\Delta x}$	Vector of corrections of the state variables in affine form.
$\widehat{\Delta y}$	Vector of corrections of the algebraic variables in affine form.
ε	Vector of noise symbols associated with AA-based power flow analysis.
εa	Vector of individual noise symbols associated with approximation errors.
ε_{AH}	Noise symbols associated with the approximation errors of the multiplication of two affine forms.
ε_H	Noise symbols associated with the approximation errors of non-affine operations.
ε_{IG}	Noise symbols associated with intermittent sources of power.
$\varepsilon_{PVa,b}$	Noise symbols associated with voltage control settings.
ε_{vs}	Vector of noise symbols associated with AA-based voltage stability assessment.
Fa	Individual approximation error of non-affine operations of $\widehat{\Delta F}$.
$\widehat{J}$	Jacobian matrix in affine form.
J_H	Equivalent approximation error for the Jacobian matrix.
Ja	Individual approximation error for the Jacobian matrix.
λ	Bifurcation parameter.
$\widehat{\lambda}$	Bifurcation parameter in affine form.
L	Vector of active and reactive power injections for the AA-based power flow analysis (p.u.).
L_{vs}	Vector of active and reactive power injections for the AA-based voltage stability assessment (p.u.).
N_h	Set of noise symbols introduced by approximations of non-affine operations.
P	Injected active power (p.u.).
$\widehat{P}$	Injected active power in affine form (p.u.).
P_G	Active power generated (p.u.).

978-1-4799-0199-9/13/ $31.00

$\widehat{P_G}$ Active power generated in affine form (p.u.).
P^{IG} Computed partial deviation of the injected active power related to intermittent sources of power (p.u.).
P^{PV} Computed partial deviation of the injected active power related to PV buses (p.u.).
P^{A} Computed partial deviation of the injected active power related to approximation errors (p.u.).
Q Injected reactive power (p.u.).
$\widehat{Q}$ Injected reactive power in affine form (p.u.).
q Matrix of errors introduced by approximations of non-affine operations in AA-based power flow analysis.
q_{vs} Matrix of errors introduced by approximations of non-affine operations in AA-based voltage stability assessment.
Q_G Reactive power generated (p.u.).
$\widehat{Q_G}$ Reactive power generated in affine form (p.u.).
Q^{IG} Computed partial deviation of the injected reactive power related to intermittent sources of power (p.u.).
Q^{PV} Computed partial deviation of the injected reactive power related to PV buses (p.u.).
Q^{A} Computed partial deviation of the injected reactive power related to approximation errors (p.u.).
R_{IC} Vector of central values for active and reactive power in AA-based power flow analysis (p.u.).
$R_{vs_{IC}}$ Vector of central values for active and reactive power in AA-based voltage stability assessment (p.u.).
θ Bus voltage angles (rad).
$\widehat{\theta}$ Affine form for bus voltage angles (rad).
$\widehat{u}$ Affine form of the variable u.
$\widehat{u_A}$ Affine form of the variable u_A.
u_{A_H} Approximation error of non-affine operations for the affine form $\widehat{u}_A$.
$\widehat{u_B}$ affine form of the variable u_B.
u_{B_H} Approximation error of non-affine operations for the affine form $\widehat{u}_B$.
u_{AB_H} Approximation error of the multiplication of the affine forms $\widehat{u}_A$ and $\widehat{u}_B$.
V Bus voltage magnitudes (p.u.).
$\widehat{V}$ Affine form for bus voltage magnitudes (p.u.).
$V_{a,b_{pv}}$ Auxiliary variables (p.u.).
V_{PQ} Variable associated with the voltage of the PQ-bus used as parameter (p.u.).
$\widehat{V_{PQ}}$ Affine form of the variable associated with the voltage of the PQ-bus used as parameter (p.u.).
x Bus voltage magnitudes, angles and other relevant unknown variables such as generator reactive powers in case of power flow equations, and state variables in case of differential-algebraic equations (p.u.).
$\widehat{x}$ Affine form of the state variables (p.u.).
y Algebraic variables such as static voltages and angles (p.u.).
$\widehat{y}$ Affine form of the algebraic variables (p.u.).

Parameters

B Susceptance matrix (p.u.).
ΔL Load changes (MW).
ΔP_G Direction of generator dispatch (p.u.).
ΔP_{G_A} Variation of generated power (p.u.).
ΔP_L Direction of the active power variations of load (p.u.).
ΔQ_L Direction of reactive power variations of load (p.u.).
ΔV_A Variation of voltage settings (p.u.).
ΔV_p Step size used in the parametrization technique (p.u.).
Δt Time step (s).
D Damping coefficient.
ε_A Noise symbols introduced by the approximation of non-affine operations.
G Conductance matrix (p.u.).
H Inertia constant (p.u.-s).
K_G Variable for representing power share in the distributed slack bus approach.
N Number of buses.
N_{DA} Number of differential-algebraic equations.
N_{IG} Set of buses with intermittent sources of power.
N_{PV} Set of PV buses.
p In case of power flow equations, this vector represents specified active and reactive powers injected at each node, as well as terminal generator voltage set points. In case of system differential equations, this vector stands for any controllable parameter. (p.u.).
P_L Active power demand (p.u.).
Q_L Reactive power demand (p.u.).
t_o Initial simulation time (s).
t_f Final computation time for time domain simulations (s).
V_p Magnitude of the voltage used as a parameter (p.u.).
V_2 Voltage magnitude of the infinite bus (p.u).
X'_d Direct axis transient reactance of the generator (p.u.).
X_T Reactance of the transformer (p.u).
X_{12} Transmission line reactance (p.u.).

Functions

f Set of power flow equations or differential equations in case of transient stability.
g Set of algebraic equations.

Introduction

Affine Arithmetic (AA) is a numerical analysis technique based on the representation of the variables as affine combinations of data uncertainties and/or approximation errors [1]. The main advantage of this technique is the possibility of tracking the correlations among variables, which is not possible for other self-validated techniques such as Interval Arithmetic (IA). This characteristic allows reducing the excessively conservative bounds that may arise with IA. AA found applications in several fields such as computer graphics [1]–[3], circuit sizing [4], and analysis under uncertainties [5]. In the area of power systems, an AA-based technique is proposed in [6] to solve the power flow problem, considering uncertainties associated with loads and generation, and hence computing the bounds of voltage profiles associated with the uncertainties. This paper proposes an AA based computing paradigm for voltage and transient stability assessment

of power systems, considering uncertainties associated with power injections, which can be associated with solar and wind generation sources.

A variety of methods can be found in the literature that address the issue of uncertainties in power systems [7]–[42]. One of the most widely used approaches is the Monte Carlo (MC) simulations [7]–[12], which accurately models system complexities but at a high computational cost, which may be prohibitive in certain applications. Aimed at reducing the computational cost of MC simulations, while achieving acceptable accuracy, several sampling and analytical approaches have been proposed in the literature. For instance, the two-point estimate method is used in [13] to compute an approximation of the moments of the system transfer capability, assuming uncertainties in power injections and transmission line parameters, based on two probability concentrations for each uncertain variable. Similarly, in [14], the two-point estimate method is used to compute the Probablity Density Function (PDF) of the maximum relative rotor angle, considering uncertainties in loads and clearing times. Although the two-point estimate method significantly reduces the computation time, as compared to MC simulations, when the number of uncertain variables and/or statistical dispersion increases, the method is not sufficiently accurate as the MC simulations [15]. Moreover, the order of the method depends on the PDF of the uncertain variables.

Linearization techniques are used in [16]–[18] to efficiently estimate the transfer capability margins due to variations in system parameters. Similarly, in [19], a method to compute the transient stability indices in terms of relevant system fixed and statistical parameters is presented. The nonlinear relationship between the critical clearing time and system load is approximated using a log-linear model whose parameters are computed by linear regression. In [20], the Potential Energy Boundary Surface method is used for probabilistic transient stability assessment considering uncertainties associated with fault clearing times and system loads. In [21], the PDF of the critical clearing time is determined using a linear function with respect to the system load, which is computed using the equal area criterion together with linearization techniques around an equilibrium point. These methods are able to estimate the voltage and transient stability indices efficiently, but within narrow limits in which the linearizations are valid.

Conditional probability based approaches are also reported in the literature for assessment of transient stability [22]–[26]. Similar to the MC simulation methods, these approaches are mainly applied to stability studies associated with medium and long term planning. Even though the conditional probability based approaches reduce the simulation times as compared to MC-based approaches, these require considerable computational effort relative to other time simulation approaches. Furthermore, these methods rely on available historical data in order to provide accurate statistics of the transient stability indices. In general, conditional probability based approaches exhibit some difficulties in properly defining the PDFs of the uncertainties associated with the operating conditions.

Some research is reported on the application of machine learning techniques for probabilistic transient stability assessment [27]–[30] and voltage stability assessment [31]–[33], to improve the computational efficiency as compared to MC-based methods. Direct intelligent search paradigms, such as Population-based Intelligent Search (PIS) have been proposed in the literature for risk assessment of power systems [34], with the aim of generating the dominant failure states and minimize the generation of success states, and hence improving the computational efficiency as compared to MC simulations.

Re-sampling based approaches are also reported in the literature. Specifically, the bootstrap method has been used as an alternative to MC simulations for empirically computing the parametric confidence intervals of a sampling distribution in power system analysis [35], [36]. Although the bootstrap method is reported to be more efficient than the MC simulations [37], in terms of computational efforts, it still requires repetitive simulations. Alternatively, a stochastic response surface is used in [38] to estimate the PDF of the loadability margins considering power injection uncertainties associated with renewable sources, while in [39], a hyper-cone model is used to compute the worst case scenario of maximum loadabilities, assuming uncertain loads.

As an alternative to sampling- and statistical-based methods, soft-computing-based techniques are proposed in the literature. For instance, in [40] and [41] fuzzy set theory is used to represent uncertainties in voltage stability assessment. In [42], fuzzy set theory is applied to determine transient stability indices for a defined number of system conditions. An important effort has been made in the literature to define the connection between interval analysis and fuzzy set theory [43]–[45]. It is stated in [45] that the theory of fuzzy information granulation, the rough set theory, and interval analysis can all be considered as subsets of a conceptual and computing paradigm of information processing, called Granular Computing.

Self-validated techniques for power system analysis are also proposed in the literature. For instance, in [46], IA is applied to compute the power flow bounds of a five-bus test system when loads and generator powers are defined by intervals. The authors observe that although the IA offers a better performance than the MC simulations in terms of computation time, it may produce excessively conservative results when the input interval sizes increase. Also, an IA based approach is proposed in [47] for transient stability assessment considering uncertainties in the system parameters. The resultant interval differential equations are solved by means of an interval Taylor series method. It is noted that the IA-based methodology leads to error explosion, as the simulation time progresses. On the other hand, a methodology to evaluate the impact of parameter variations in the transient and DC response of analog circuits using AA is proposed in [48]. This methodology solves a set of Differential Algebraic Equations (DAEs) that models the analog circuit using an iterative approach. Thus, a similar AA approach is proposed here for the solution of DAEs for transient stability analysis, since this method avoids the error

explosion attributed to IA based methodologies, and represents a computationally efficient alternative to probabilistic and sampling-based techniques.

The proposed AA-based methods efficiently compute the hull of full PV curves and time domain dynamic responses of the system under uncertainties, representing useful tools to avoid insecure system operation. Unlike most of the previously discussed approaches, the uncertain variables in the proposed AA-based methods are modeled as intervals with no assumptions regarding their probabilities. This characteristic is important when the uncertainties are due to intermittent renewable sources, since the PDF of the forecasting error depends on the time horizon and the prediction method, among other factors. Furthermore, contrary to machine learning and direct search paradigms, the training, sampling, or evolutionary computational processes are not required in the AA-based techniques.

The rest of this paper is organized as follows: The second section discusses the AA-based power flow method, which is the basis for the formulation of the AA-based voltage stability analysis method proposed in the third section. In the fourth section, the proposed AA-based transient stability method is presented. The fifth section discusses the results of applying the proposed methods using two test systems. Finally, in the last section, the main conclusions and contributions of the present work are presented.

AA-based Power Flow Analysis

An AA-based technique to solve the power flow problem considering uncertainties in load and generation is proposed in [6]. Based on this approach, the bus voltages and angles in affine form can be written as:

$$\widehat{V_i} = V_{IC_i} + \sum_{m\in N_{IG}} \left.\frac{\partial V_i}{\partial P_{G_m}}\right|_{IC} \Delta P_{G_{A}m}\varepsilon_{IGm} + \sum_{c\in N_{PV}} \left.\frac{\partial V_i}{\partial V_c}\right|_{IC} \Delta V_{A_c}(\varepsilon_{PVac} - \varepsilon_{PVbc}) \tag{1}$$

$$\widehat{\theta_i} = \theta_{IC_i} + \sum_{m\in N_{IG}} \left.\frac{\partial \theta_i}{\partial P_{G_m}}\right|_{IC} \Delta P_{G_{A}m}\varepsilon_{IGm} + \sum_{c\in N_{PV}} \left.\frac{\partial \theta_i}{\partial V_c}\right|_{IC} \Delta V_{A_c}(\varepsilon_{PVac} - \varepsilon_{PVbc}) \tag{2}$$

where the noise symbols ε_{PVa} and ε_{PVb} are additional noise symbols introduced to account for the reactive power limits of generators, and thus avoid the need for PV-PQ bus switching of the power flow AA formulation used in [6]. This approach is based on the representation of PV buses discussed in [49]. The voltage at PV buses is defined as:

$$V_c = V_{IC_c} + \Delta V_{A_c}\varepsilon_{PVac} - \Delta V_{A_c}\varepsilon_{PVbc} \qquad \forall c \in N_{PV} \tag{3}$$

where:

$$\begin{aligned} &0 \le \varepsilon_{PVac} \le 1, \varepsilon_{PVbc} = 0 \quad \text{for} \quad Q_G < Q_{G_{min}} \\ &\varepsilon_{PVac} = 0, 0 \le \varepsilon_{PVbc} \le 1 \quad \text{for} \quad Q_G > Q_{G_{max}} \qquad \forall c \in N_{PV} \\ &\varepsilon_{PVac} = 0, \varepsilon_{PVbc} = 0 \quad \text{for} \quad Q_{G_{max}} \le Q_G \le Q_{G_{min}} \end{aligned} \tag{4}$$

The first condition in (4) guarantees that the minimum reactive power constraint of the generator is not violated. This is achieved by increasing the magnitude of the reference voltage by means of the auxiliary variable ε_{PVac} according to (3). Similarly, the second condition avoids violation of the upper reactive power limit by adjusting the magnitude of the auxiliary variable ε_{PVbc}, which reduces the reference voltage of the generator. When no reactive power limits are violated, the auxiliary variables in (3) are zero as in the third condition, thus keeping the voltage reference at its pre-established value. The effect of the variation of the voltage specified at PV nodes due to these noise symbols is accounted for in (1) and (2) by means of the partial derivatives of the bus voltages and angles, with respect to the voltage reference set points at PV buses. This approach is implemented using the Linear Programming (LP) formulations described in detail at the end of this section.

The coefficients of the noise symbols in (1) and (2), given by the partial derivatives of voltage magnitudes and angles with respect to the injected active power and reference voltages at voltage controlled buses, can be calculated from a "base" power flow solution and its associated Jacobian matrix. These derivates are evaluated at the following central values of the active powers injected at buses where intermittent generators are considered:

$$P_{G_{IC}m} = \frac{P_{G_{max}m} + P_{G_{min}m}}{2} \qquad \forall m \in N_{IG} \tag{5}$$

The active and reactive power affine forms $\widehat{P_i}$ and $\widehat{Q_i}$ are obtained by replacing the voltage and angle affine forms given in (1) and (2) in the following equations $\forall i = 1, .., N$:

$$\widehat{P_i} = \sum_{j=1}^{N} \widehat{V_i}\widehat{V_j}[G_{ij}\cos(\widehat{\theta_i} - \widehat{\theta_j}) + B_{ij}\sin(\widehat{\theta_i} - \widehat{\theta_j})] \tag{6}$$

$$\widehat{Q_i} = \sum_{j=1}^{N} \widehat{V_i}\widehat{V_j}[G_{ij}\sin(\widehat{\theta_i} - \widehat{\theta_j}) - B_{ij}\cos(\widehat{\theta_i} - \widehat{\theta_j})] \tag{7}$$

Since the sinusoidal functions are non-affine operations, they are expanded in this paper in terms of a series of Chebyshev polynomials for five digits accuracy [50].

The affine form for the active power equations (6) and reactive power equations (7) exhibit the following form, after all affine function operations and approximations given in [1], [2]:

$$\widehat{P_i} = P_{i_{IC}} + \sum_{m\in N_{IG}} P^{IG}_{i,m}\varepsilon_{IG_m} + \sum_{c\in N_{PV}} P^{PV}_{i,c}\varepsilon_{PV_{a_c}} - \sum_{c\in N_{PV}} P^{PV}_{i,c}\varepsilon_{PV_{b_c}} + \sum_{h\in N_h} P^{A}_{i,h}\varepsilon_{A_h} \tag{8}$$

$$\widehat{Q_i} = Q_{i_{IC}} + \sum_{m\in N_{IG}} Q^{IG}_{i,m}\varepsilon_{IG_m} + \sum_{c\in N_{PV}} Q^{PV}_{i,c}\varepsilon_{PV_{a_c}} - \sum_{c\in N_{PV}} Q^{PV}_{i,c}\varepsilon_{PV_{b_c}} + \sum_{h\in N_h} Q^{A}_{i,h}\varepsilon_{A_h} \tag{9}$$

These equations may be written in compact form as follows:

$$A\varepsilon = C \tag{10}$$

$$C = L - (R_{IC} + q) \tag{11}$$

where:

$$A = \begin{bmatrix} P^{IG}_{1,1} & \cdots & P^{IG}_{1,N_{IG}} & P^{PV}_{1,1} & \cdots & P^{PV}_{1,N_{PV}} & -P^{PV}_{1,1} & \cdots & -P^{PV}_{1,N_{PV}} \\ \vdots & \vdots & \vdots & \vdots & \vdots & \vdots & \vdots & \vdots & \vdots \\ P^{IG}_{N-1,1} & \cdots & P^{IG}_{N-1,N_{IG}} & P^{PV}_{N-1,1} & \cdots & P^{PV}_{N-1,N_{PV}} & -P^{PV}_{N-1,1} & \cdots & -P^{PV}_{N-1,N_{PV}} \\ Q^{IG}_{1,1} & \cdots & Q^{IG}_{1,N_{IG}} & Q^{PV}_{1,1} & \cdots & Q^{PV}_{1,N_{PV}} & -Q^{PV}_{1,1} & \cdots & -Q^{PV}_{1,N_{PV}} \\ \vdots & \vdots & \vdots & \vdots & \vdots & \vdots & \vdots & \vdots & \vdots \\ Q^{IG}_{N-1,1} & \cdots & P^{IG}_{N-1,N_{IG}} & Q^{PV}_{N-1,1} & \cdots & P^{PV}_{N-1,N_{PV}} & -Q^{PV}_{N-1,1} & \cdots & -Q^{PV}_{N-1,N_{PV}} \end{bmatrix}$$

$$\varepsilon = \begin{bmatrix} \varepsilon_{IG_1} \\ \vdots \\ \varepsilon_{IG_{N_{IG}}} \\ \varepsilon_{PV_{a,1}} \\ \vdots \\ \varepsilon_{PV_{a,N_{PV}}} \\ \varepsilon_{PV_{b,1}} \\ \vdots \\ \varepsilon_{PV_{b,N_{PV}}} \end{bmatrix} \qquad L = \begin{bmatrix} [P_{G_{min_1}} - P_{L_1}], [P_{G_{max_1}} - P_{L_1}] \\ \vdots \\ [P_{G_{min_{N-1}}} - P_{L_{N-1}}], [P_{G_{max_{N-1}}} - P_{L_{N-1}}] \\ [Q_{G_{min_1}} - Q_{L_1}], [Q_{G_{max_1}} - Q_{L_1}] \\ \vdots \\ [Q_{G_{min_{N-1}}} - Q_{L_{N-1}}], [Q_{G_{max_{N-1}}} - Q_{L_{N-1}}] \end{bmatrix}$$

$$R_{IC} = \begin{bmatrix} P_{1_{IC}} \\ \vdots \\ P_{N_{IC}} \\ Q_{1_{IC}} \\ \vdots \\ Q_{N_{IC}} \end{bmatrix} \qquad q = \begin{bmatrix} P^A_{1,1} & \cdots & P^A_{1,Nh} \\ \vdots & \vdots & \vdots \\ P^A_{N-1,1} & \cdots & P^A_{N-1,Nh} \\ Q^A_{1,1} & \cdots & Q^A_{1,Nh} \\ \vdots & \vdots & \vdots \\ Q^A_{N-1,1} & \cdots & Q^A_{N-1,Nh} \end{bmatrix} \begin{bmatrix} \varepsilon a_1 \\ \vdots \\ \vdots \\ \vdots \\ \vdots \\ \varepsilon a_{N_h} \end{bmatrix}$$

To obtain the maximum and minimum values of the noise vector ε in (10), the following LP problems must be solved:

$$\begin{aligned} \min \quad & \textstyle\sum \varepsilon_{IG_{min}m} + \sum \varepsilon_{PVa_{min}c} + \sum \varepsilon_{PVb_{min}c} \\ \text{s.t.} \quad & -1 \le \varepsilon_{IG_{min}m} \le 1 \\ & 0 \le \varepsilon_{PVa_{min}c}, \varepsilon_{PVb_{min}c} \le 1 \\ & C_{min} \le A\varepsilon_{min} \le C_{max} \\ & \forall m \in N_{IG}, \forall c \in N_{PV} \end{aligned} \tag{12}$$

$$\begin{aligned} \max \quad & \textstyle\sum \varepsilon_{IG_{max}m} + \sum \varepsilon_{PVa_{max}c} + \sum \varepsilon_{PVb_{max}c} \\ \text{s.t.} \quad & -1 \le \varepsilon_{IG_{max}m} \le 1 \\ & -1 \le \varepsilon_{PVa_{max}c}, \varepsilon_{PVb_{max}c} \le 0 \\ & C_{min} \le A\varepsilon_{max} \le C_{max} \\ & \forall m \in N_{IG}, \forall c \in N_{PV} \end{aligned} \tag{13}$$

The values of $\varepsilon_{IG_{min}}$, $\varepsilon_{PVa_{min}}$, $\varepsilon_{PVb_{min}}$, and $\varepsilon_{IG_{max}}$, $\varepsilon_{PVa_{max}}$, $\varepsilon_{PVb_{max}}$ obtained by solving these simple LP problems are used in (1) and (2) to compute the maximum and minimum bus voltages and angles. Notice that the objective functions in (12) and (13) are mathematically formulated to contract the vector ε according to the physical restrictions imposed by the power flow equations and the bounds of the noise symbols. Thus, there is no particular physical meaning attributed to the objective funtions.

AA-based Computation of PV Curves

Voltage stability is associated with the ability of the power system to maintain acceptable voltage levels under normal operating conditions and after the system is perturbed by small or large disturbances. Although voltage stability is a dynamic process, the absence of the post-contingency long-term equilibrium, which is associated with voltage collapse, can be analyzed using steady-state analysis techniques [51], [52].

The maximum loadability before the system experiences a voltage collapse, which is characterized by a progressive fall of bus voltage magnitudes, is associated with the existence of a saddle node or limit-induced bifurcation [51]. The saddle node bifurcation is identified as the operating point where the system state matrix is singular, which usually results in no power flow solutions due to the singularity of the power flow Jacobian matrix. Limit-induced bifurcations refer to an operating point where generators reach their reactive power limits and lose their voltage control capability, which may also result in no power flow solutions.

The maximum loadability and voltage profiles as the loading changes are commonly computed using the continuation power flow technique [53]–[55]. This technique is based on the solution of power flow equations that can be represented by:

$$f_{PF}(x_{PF}, p_{PF}, \lambda) = 0 \tag{14}$$

The parameter λ is used to generate different scenarios for loads and generator outputs as follows:

- For generator powers excluding the slack bus:

$$P_{Gi}(\lambda) = P_{Goi} + \lambda\Delta P_{Gi} \qquad \forall i = 1, ..., N-1 \tag{15}$$

- For generator powers including the slack bus (distributed slack bus):

$$P_{Gi}(\lambda) = P_{Goi} + (\lambda + K_G)\Delta P_{Gi} \qquad \forall i = 1, ..., N \tag{16}$$

- For load powers:

$$P_{Li}(\lambda) = P_{Loi} + \lambda\Delta P_{Li} \qquad \forall i = 1, ..., N \tag{17}$$

$$Q_{Li}(\lambda) = Q_{Loi} + \lambda\Delta Q_{Li} \qquad \forall i = 1, ..., N \tag{18}$$

The solutions of (14) for different values of λ are obtained using predictor and corrector steps [51]. Solutions obtained from the continuation power flow yield PV curves and the maximum system loadability, which is commonly used to compute voltage stability margins.

Equation (15) can be written in AA as follows:

$$\widehat{P}_{G_i}(\lambda) = P_{G_{oi}} + \widehat{\lambda}\Delta P_{Gi} \qquad \forall i = 1, .., N-1 \tag{19}$$

Similarly, the load equations can be written as:

$$\widehat{P}_{L_i}(\lambda) = P_{L_{oi}} + \widehat{\lambda}\Delta P_{Li} \qquad \forall i = 1, .., N \tag{20}$$

$$\widehat{Q}_{L_i}(\lambda) = Q_{L_{oi}} + \widehat{\lambda}\Delta Q_{Li} \qquad \forall i = 1, .., N \tag{21}$$

where:

$$\widehat{\lambda} = \lambda_{IC} + \sum_{m\in N_{IG}} \frac{\partial\lambda}{\partial P_{G_m}}\bigg|_{IC} \Delta P_{G_{A}m}\varepsilon_{IGm} + \sum_{c\in N_{PV}} \frac{\partial\lambda}{\partial V_c}\bigg|_{IC} \Delta V_c(\varepsilon_{PVac} - \varepsilon_{PVbc}) \tag{22}$$

Notice that the loading parameter λ is now in affine form, and thus is written as a function of the variability of the output power of intermittent generators. This variability is modeled as intervals that represent the maximum and minimum power injections associated with the simulation time period as follows:

$$P_{G_m} = [P_{G_{IC}m} - \Delta P_{G_{A}m}, P_{G_{IC}m} + \Delta P_{G_{A}m}] \qquad \forall m \in N_{IG} \tag{23}$$

or equivalently in AA:

$$\widehat{P}_{G_m} = P_{G_{IC}m} + \Delta P_{G_{A}m}\varepsilon_{IGm} \qquad \forall m \in N_{IG} \tag{24}$$

For a different period of time, a different interval for the uncertain power injections may be needed; for instance, ΔP_{G_A} may be chosen according to the forecasting error associated with the concerned planning horizon. On the other hand, ΔV_c may be decided so that there is a sufficient margin for the variation of the reference voltage setting of PV buses in order to keep generator's reactive power within limits. In this paper, ΔV_c has been assumed to be a 10% of the pre-established reference voltage control settings for all study cases. The affine forms for voltages and angles can be written as in (1) and (2). For the computation of the central values and the upper and lower bounds of the PV curves, a parametrization technique is used in this paper. Figure 1(a) illustrates the problems when the load power is used as a parameter to compute the lower and upper parts of the PV curves. Note that varying the load by varying the power from P_{L1} to P_{L7}, and computing the respective upper voltages V_{u1} to V_{u7} and lower voltages V_{l1} to V_{l7} based on AA or MC simulations can only be done until the lower bound of the PV curve reaches the maximum loading point given by P_{L7}. Beyond this point, the dotted parts of the PV curves cannot be readily computed. To overcome this problem, the voltage magnitude at a PQ bus is chosen as the parameter, as in Fig. 1(b), based on a parametrization approach [51], [53]–[55]. Notice that the voltage magnitude at the chosen PQ bus varies from V_1 to V_9, and for each of these voltages, the associated lower power loads P_{Ll1} to P_{Ll9} and upper power loads P_{Lu1} to P_{Lu9} can be readily computed. The PQ-bus voltage of the bus that exhibits the largest variation in voltage magnitude with respect to load variations is used as the parameter. The affine form for the voltage of this bus can be written as:

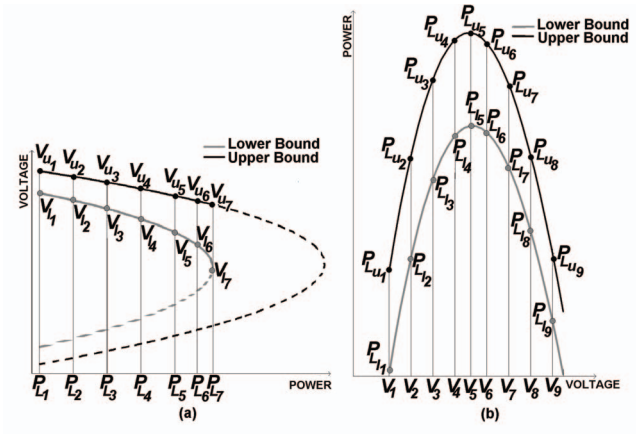

Fig. 1. PV curves: (a) using the load power as the parameter; (b) using a PQ-bus voltage magnitude as the parameter.

$$\widehat{V}_{PQ} = V_p \tag{25}$$

where V_p is updated for the computation of the PV curves as follows:

$$V_p = V_p - \Delta V_p \tag{26}$$

The step size ΔV_p varies depending on the proximity to the maximum loadability; thus, the closer to this maximum, the smaller the step size. The proximity to maximum loadability is detected by computing the difference between the former and the actual loading factor λ; the lower this difference, the closer the system is to a saddle node or limit-induced bifurcation. Notice that for computations beyond the maximum loadability, the loading factor starts decreasing, and thus it is straightforward to detect when the maximum loadability has been reached.

The proposed PV-curve computation approach is based on the following AA form of power flow equations:

$$\widehat{P}_{G_i} - P_{L_{oi}} - \widehat{\lambda}\Delta P_{Li} - \widehat{P}_i = 0 \qquad \forall i = 1, ..., N \tag{27}$$

$$\widehat{Q}_{G_i} - Q_{L_{oi}} - \widehat{\lambda}\Delta Q_{Li} - \widehat{Q}_i = 0 \qquad \forall i = 1, ..., N \tag{28}$$

plus the additional equation (25) corresponding to the parametrization approach. Here, $\widehat{P}_i$ and $\widehat{Q}_i$ are written according to (8) and (9), and $\widehat{P}_{G_i}$ is given by (19) for dispatchable generators, excluding the slack bus. In case of non-dispatchable generators, $\widehat{P}_{G_i}$ is modeled as an interval which represents the uncertainties associated with the output power, as in (24).

Equations (27) and (28) exhibit the following compact form,

after all affine function operations and approximations:

$$A_{vs}\varepsilon_{vs} = C_{vs} \tag{29}$$

$$C_{vs} = L_{vs} - (R_{vs_{IC}} + q_{vs}) \tag{30}$$

where:

$$R_{vs_{IC}} = \begin{bmatrix} P_{1_{IC}} + \lambda_{IC}(\Delta P_{L_1} - \Delta P_{G_1}) \\ \vdots \\ P_{N_{IC}} + \lambda_{IC}(\Delta P_{L_N} - \Delta P_{G_N}) \\ Q_{1_{IC}} + \lambda_{IC}\Delta Q_{L_1} \\ \vdots \\ Q_{N_{IC}} + \lambda_{IC}\Delta Q_{L_N} \end{bmatrix}$$

and A_{vs}, ε_{vs}, C_{vs}, L_{vs}, and q_{vs} have the form of the matrices used in (10) and (11).

Using a similar approach to the one described in the previous section, the LP formulation for the proposed AA based voltage stability assessment is obtained by substituting C by C_{vs} and A by A_{vs} in (12) and (13). The values for $\varepsilon_{IG_{min}}$, $\varepsilon_{PVa_{min}}$, $\varepsilon_{PVb_{min}}$, and $\varepsilon_{IG_{max}}$, $\varepsilon_{PVa_{max}}$, $\varepsilon_{PVb_{max}}$ obtained by solving the resultant LP formulations are used in (22) to compute the minimum and maximum values of λ.

AA-based Method for Transient Stability Assessment

Transient stability is associated with the ability of the power system to remain in synchronism when subjected to a large and sudden disturbance. The severity of this disturbance makes it impossible to linearize the system dynamic equations; thus, in practical systems, numerical integration techniques are commonly used to solve these nonlinear equations. The general form for the non-linear differential algebraic equations (DAEs) that describe the system behavior is as follows:

$$\dot{x}_D(t) = f_D(x_D, y, p_D, \lambda) \qquad x_D(t_o) = x_{D_o} \tag{31}$$

$$0 = g(x_D, y, p_D, \lambda) \qquad y(t_o) = y_o \tag{32}$$

where x_D represents the state variables such as generator internal angles and speeds; y refers to algebraic variables such as static voltages and angles; p_D stands for controllable parameters such as AVR set points; and λ represents uncontrollable parameters such as load levels. A different set of (31) and (32) is needed whenever a discrete variable changes; this accounts for the possible discontinuities in the algebraic variables that occur, for instance, when a transmission line is tripped. In this case, the algebraic variables after and before the line trip time instant describe continuous trajectories, with a discontinuity at the line trip time instant. These algebraic variables are, therefore, allowed to change instantaneously, which is not the case for the state variables that always describe continuous trajectories.

The set (31) and (32) can be formulated in AA as follows:

$$\dot{\widehat{x}}_D(t) = f_D(\widehat{x}_D, \widehat{y}, \widehat{p}_D, \widehat{\lambda}) \qquad \widehat{x}_D(t_o) = \widehat{x}_{D_o} \tag{33}$$

$$0 = g(\widehat{x}_D, \widehat{y}, \widehat{p}_D, \widehat{\lambda}) \qquad \widehat{y}(t_o) = \widehat{y}_o \tag{34}$$

The purpose of this formulation is to compute the hull of the system response due to intermittent sources of power when large disturbances occur. To achieve this goal, the set of differential-algebraic equations in affine form are solved by using a trapezoidal integration approach, resulting in the following formulation for the differential equations:

$$\widehat{x}_{D_n} - \widehat{x}_{D_{n-1}} + (\Delta t/2)(f_D(\widehat{x}_{D_{n-1}}, \widehat{y}_{n-1}, \widehat{p}_D, \widehat{\delta}, t_{n-1}) + f_D(\widehat{x}_{D_n}, \widehat{y}_n, \widehat{p}_D, \widehat{\delta}, t_n)) = 0 \tag{35}$$

The initial affine forms of the state and algebraic variables are computed as:

$$\widehat{x_D} = x_{D_{IC}} + \sum_{m \in N_{IG}} \left.\frac{\partial x_D}{\partial P_{G_{A_m}}}\right|_{IC} \Delta P_{G_{A_m}} \varepsilon_{IG_m} \tag{36}$$

$$\widehat{y} = y_{IC} + \sum_{m \in N_{IG}} \left.\frac{\partial y}{\partial P_{G_{A_m}}}\right|_{IC} \Delta P_{G_{A_m}} \varepsilon_{IG_m} \tag{37}$$

The central values are computed by solving the following set of steady-state equations:

$$f_D(x_{D_{IC}}, y_{IC}, p_{D_{IC}}, \delta_{IC}) = 0 \tag{38}$$

$$g(x_{D_{IC}}, y_{IC}, p_{D_{IC}}, \delta_{IC}) = 0 \tag{39}$$

$$P_{G_{IC_m}} = \frac{P_{G_{max_m}} + P_{G_{min_m}}}{2} \qquad \forall m \in N_{IG} \tag{40}$$

and the affine forms of the intermittent sources of power are modeled as in (24).

The resultant set of algebraic equations can be solved using a Newton approach as follows:

$$\widehat{\Delta F} = \widehat{J}\widehat{\Delta X} \tag{41}$$

This linear system of equations is solved iteratively, updating the state and algebraic variables until convergence is attained. According to this formulation, the set of differential and algebraic equations are simultaneously solved, achieving better numerical stability than partitioned techniques. The components of the vector $\widehat{\Delta F}$ in (41) exhibits the following form after all affine functions and approximations:

$$\widehat{\Delta F_s} = \Delta F_{IC_s} + \Delta F_{1_s}\varepsilon_{IG_1} + \Delta F_{2_s}\varepsilon_{IG_2} + ... + \Delta F_{m_s}\varepsilon_{IG_m} + \sum_{h \in Nh} (Fa_{h_s})\varepsilon_{H_{h,s}} = 0 \quad \forall m \in N_{IG}, \quad s = 1...N_{DA} \tag{42}$$

The last term of this equation, which corresponds to the independent noise symbols that results from the non-affine operations can be reduced into a single noise symbol as follows:

$$\sum_{h\in Nh} |(Fa_{h_s})|\varepsilon_{H_{h,s}} = \Delta F_{H_s}\varepsilon_{H_s} \quad s = 1...N_{DA} \tag{43}$$

Similarly, the components of the Jacobian matrix can be written as:

$$\widehat{J}_{s,j} = J_{IC_{s,j}} + J_{1_{s,j}}\varepsilon_{IG_1} + J_{2_{s,j}}\varepsilon_{IG_2} + ... + J_{m_{s,j}}\varepsilon_n + J_{H_{s,j}}\varepsilon_{H_s} \quad \forall m \in N_{IG} \quad s, j = 1...N_{DA} \tag{44}$$

$$J_{H_{s,j}} = \sum_{h\in Nh} |(Ja_{h_{s,j}})|\varepsilon_{H_s} \quad s, j = 1...N_{DA} \tag{45}$$

and the affine forms of the vector $\widehat{\Delta X}$ are:

$$\widehat{\Delta X_s} = \Delta X_{IC_s} + \Delta X_{1_s}\varepsilon_{IG_1} + ... + \Delta X_{m_s}\varepsilon_{IG_m} + \Delta X_{H_s}\varepsilon_{H_s} \quad s = 1...N_{DA}, \forall m \in N_{IG} \tag{46}$$

This vector is comprised of the state and algebraic variables, and thus have the following form:

$$\widehat{\Delta X} = \begin{bmatrix} \widehat{\Delta x} \\ \widehat{\Delta y} \end{bmatrix} \tag{47}$$

The multiplication of the affine forms in (41) can be defined as follows:

$$\widehat{u} = \widehat{u_A}\widehat{u_B} = u_{A_{IC}}u_{B_{IC}} + \sum_{m\in N_{IG}} (u_{A_{IC}}u_{B_m} + u_{B_{IC}}u_{A_m})\varepsilon_{IG_m} + (u_{A_{IC}}u_{B_H} + + u_{B_{IC}}u_{A_H})\varepsilon_H + u_{AB}\varepsilon_{AH} \tag{48}$$

where $\widehat{u_A}$ and $\widehat{u_B}$ are two different affine variables. This yields the following components of the affine form $\widehat{\Delta F}$:

- Central values:

$$\Delta F_{IC_s} = \sum_{j=1}^{N_{DA}} J_{IC_{s,j}}\Delta X_{IC_j} \quad s = 1...N_{DA} \tag{49}$$

- The m-th components:

$$\Delta F_{m_s} = \sum_{j=1}^{N_{DA}} J_{IC_j}\Delta X_{m_j} + \sum_{j=1}^{N_{DA}} J_{m_{s,j}}\Delta X_{IC_j} \quad s = 1...N_{DA}, \forall m \in N_{IG} \tag{50}$$

- Approximation errors:

$$\Delta F_{H_s} = \sum_{j=1}^{N_{DA}} J_{IC_{s,j}}\Delta X_{H_j} + \sum_{j=1}^{N_{DA}} J_{H_{s,j}}\Delta X_{IC_j} \quad s = 1..N_{DA}, \forall m \in N_{IG} \tag{51}$$

These equations are used to compute the components of the affine form $\widehat{\Delta X}$ according to the following formulations in matrix form:

$$\begin{bmatrix} \Delta F^r_{IC_1} \\ \Delta F^r_{IC_2} \\ \vdots \\ \Delta F^r_{IC_{N_{DA}}} \end{bmatrix} = \begin{bmatrix} J^r_{IC_{1,1}} & J^r_{IC_{1,2}} & \cdots & J^r_{IC_{1,N_{DA}}} \\ J^r_{IC_{2,1}} & J^r_{IC_{2,2}} & \cdots & J^r_{IC_{2,N_{DA}}} \\ \vdots & \vdots & \cdots & \vdots \\ J^r_{IC_{N_{DA},1}} & J^r_{IC_{N_{DA},2}} & \cdots & J^r_{IC_{N_{DA},N_{DA}}} \end{bmatrix} \begin{bmatrix} \Delta X^r_{IC_1} \\ \Delta X^r_{IC_2} \\ \vdots \\ \Delta X^r_{IC_{N_{DA}}} \end{bmatrix} \tag{52}$$

$$\begin{bmatrix} \Delta F^r_{m_1} - \Delta X^r_{IC_1}J^r_{m_{1,1}} - \ldots - \Delta X^r_{IC_{N_{DA}}}J^r_{m_{1,N_{DA}}} \\ \Delta F^r_{m_2} - \Delta X^r_{IC_1}J^r_{m_{2,1}} - \ldots - \Delta X^r_{IC_{N_{DA}}}J^r_{m_{2,N_{DA}}} \\ \Delta F^r_{m_{N_{DA}}} - \Delta X^r_{IC_1}J^r_{m_{N_{DA},1}} - \ldots - \Delta X^r_{IC_{N_{DA}}}J^r_{m_{N_{DA},N_{DA}}} \end{bmatrix} = A^r_{IC} \begin{bmatrix} \Delta X^r_{m_1} \\ \Delta X^r_{m_2} \\ \vdots \\ \Delta X^r_{m_{N_{DA}}} \end{bmatrix} \quad \forall m \in N_{IG} \tag{53}$$

$$\begin{bmatrix} \Delta F^r_{H_1} - \Delta X^r_{IC_1}J^r_{H_{1,1}} \ldots - \Delta X^r_{IC_{N_{DA}}}J^r_{H_{1,N_{DA}}} \\ \Delta F^r_{H_2} - \Delta X^r_{IC_1}J^r_{H_{2,1}} - \ldots - \Delta X^r_{IC_{N_{DA}}}J^r_{H_{2,N_{DA}}} \\ \Delta F^r_{H_{N_{DA}}} - \Delta X^r_{IC_1}J^r_{H_{N_{DA},1}} - \ldots - \Delta X^r_{IC_{N_{DA}}}J^r_{H_{N_{DA},N_{DA}}} \end{bmatrix} = A^r_{IC} \begin{bmatrix} \Delta X^r_{H_1} \\ \Delta X^r_{H_2} \\ \vdots \\ \Delta X^r_{H_{N_{DA}}} \end{bmatrix} \tag{54}$$

where the matrix A_{IC} is:

$$A^r_{IC} = \begin{bmatrix} J^r_{IC_{1,1}} & J^r_{IC_{1,2}} & \cdots & J^r_{IC_{1,N_{DA}}} \\ J^r_{IC_{2,1}} & J^r_{IC_{2,2}} & \cdots & J^r_{IC_{2,N_{DA}}} \\ \vdots & \vdots & \cdots & \vdots \\ J^r_{IC_{N_{DA},1}} & J^r_{IC_{N_{DA},2}} & \cdots & J^r_{IC_{N_{DA},N_{DA}}} \end{bmatrix} \tag{55}$$

The state and algebraic variables are iteratively updated as follows:

$$\widehat{x^{r+1}_D} = \widehat{x^r_D} + \widehat{\Delta x^r_D} \tag{56}$$

$$\widehat{y^{r+1}} = \widehat{y^r} + \widehat{\Delta y}^r \tag{57}$$

where $\Delta\widehat{y^r}$ and $\Delta\widehat{x^r_D}$ are computed using (49)-(55) These variables are iteratively updated until convergence is attained. Figure 2 illustrates the proposed algorithm for the AA-based transient stability assessment. This algorithm is very similar to the commonly used approach to solve the differential-algebraic equations for time domain simulations, but in affine form.

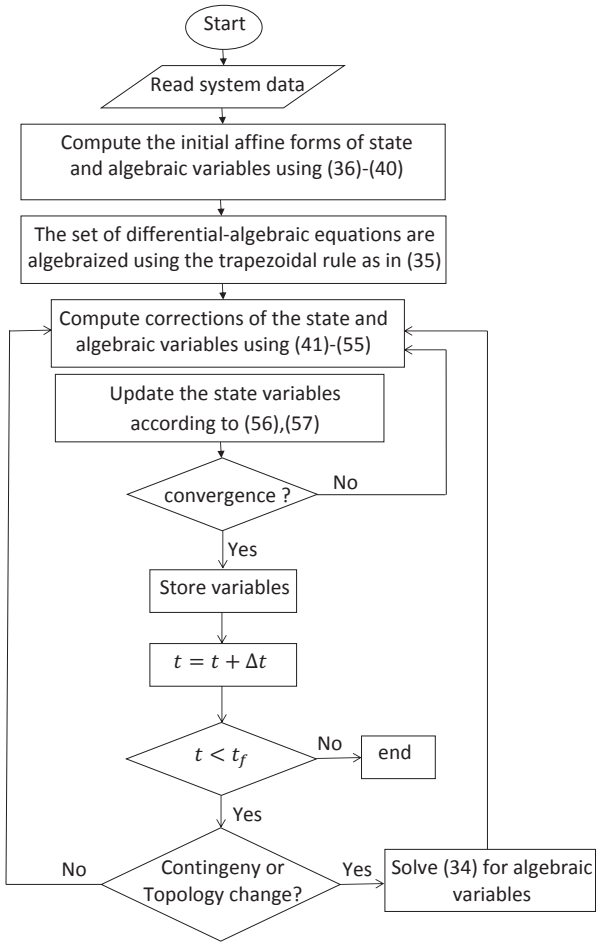

Fig. 2. AA-based time domain simulation algorithm.

Simulation Results and Disussions

To test the proposed AA-based methodologies for voltage and transient stability assessment, a 5-bus test system [56] and a generator-infinite bus test system [57] are used, respectively, as explained below. For comparison purposes, computation of PV curves and time domain simulations are performed using an MC simulation approach, assuming uniform distribution for the non-dispatchable generators intervals, and are thus treated as the benchmarks for comparison purposes. The convergence of the MC simulations was determined by assuming a tolerance of 0.0001 in the change of the expected value. These simulations, based on MATLAB, were carried out on a computer with 8 GB of RAM and a processor of 3.40 GHz.

5-Bus Test System

This system comprises two generators which supply a base load of 440 MW. One of these generators is assumed to be an intermittent power source, while the second is assumed to be dispatchable, and is the system's slack bus. For the computation of PV curves, the load directions in (20) and (21) are defined as: $\Delta P_{L_i} = P_{L_{oi}}$, $\Delta Q_{L_i} = Q_{L_{oi}}$, and the generator direction in (19) is: $\Delta P_{G_i} = P_{G_{oi}}$.

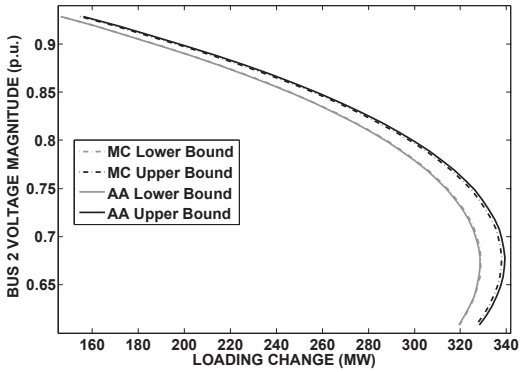

Fig. 3. PV curves for the IEEE 5-bus test system.

Figure 3 shows the PV curves obtained using MC simulations and the proposed AA methodology for a 30% margin variation of the uncertain variable. Notice that the AA approach allows efficiently computing the upper and lower bounds of the PV curves, providing information regarding the hull of voltage profiles. No other technique proposed in the literature so far can quickly generate such curves, which could be used by power system operators like standard PV curves are used now [51] (e.g. to determine voltage profiles as the maximum system loadability is approached). The proposed AA approach is computationally more efficient than MC simulations, achieving 49.03% (0.889 s vs 1.744 s) savings in computational time. The maximum loadability obtained using MC simulations and the AA-based method exhibits a difference of 0.41% and 0.12% for the upper and lower bounds, respectively. Therefore, the proposed AA-based method is able to accurately determine the PV-curves at significant computational savings.

Generator-Infinite Bus Test System

The system shown in Fig. 4 comprised of a synchronous generator, which is assumed to be intermittent, and connected through a transformer and two parallel lines to an infinite bus, is used here to demonstrate and test the proposed AA-based transient stability simulation approach. The data for this system is given in Table I. A three phase fault is assumed in the middle of one of the lines connected between Buses 1 and 2, which is subsequently cleared by tripping the faulted line. The initial central values for the affine forms are computed assuming that the infinite bus is drawing 5.5 p.u. real power at unitary p.f.

In this example, generators are modeled using a classical model; however, it is important to point out that the proposed AA-based algorithm for transient stability assessment is not model-dependent, thus, any detailed model for the power system components such as synchronous generators, wind farms and solar PV arrays can be used.

Figure 5 shows the upper and lower bounds of the system dynamic response when the intermittent source varies within the interval defined by [522.5 577.5]MW, i.e. a ±5% variation.

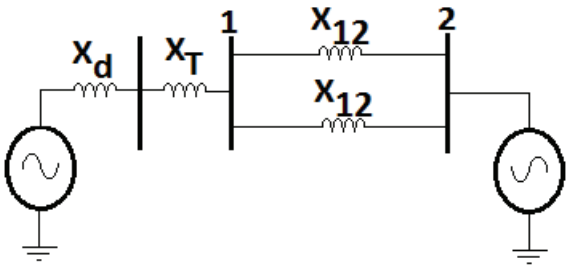

Fig. 4. Generator-Infinite Bus Test System

TABLE I
GENERATOR-INFINITE BUS TEST SYSTEM DATA

H (s)	D $(p.u)$	X'_d $(p.u.)$	X_T $(p.u.)$	X_{12} $(p.u.)$	V_2 $(p.u)$	$p.f.$	$P_{G_{IC}}$ $(p.u.)$
20.0	0.1	0.025	0.025	0.1	1.0	1	5.5

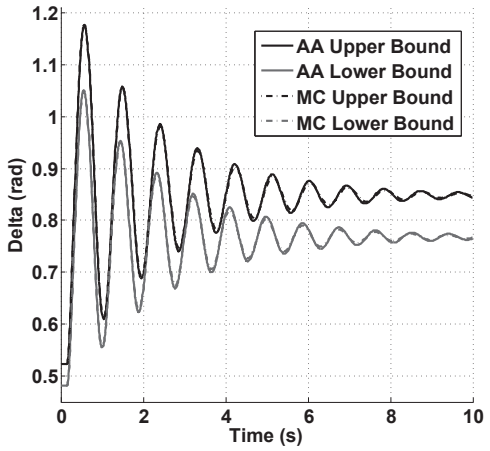

Fig. 5. Generator-Infinite Bus Test System: 3-cycle fault and ±5% variation in generation

Notice that the bounds obtained using the AA-based approach closely follows the bounds obtained using MC simulations, with a maximum error of 1%.

Figure 6 depicts the effect of the size of the interval that models the intermittent source of power on the accuracy of the proposed AA-based technique. In this case, the interval considered is [495 605]MW, i.e ±10% variation, resulting in an error of 3.97% when compared to MC simulations; thus, as the size of the interval that models the uncertain variables increases, the error increases as well, as expected. Also notice that the AA based approach is slightly conservative as compared to the MC simulations.

Figure 7 illustrates a case where the system becomes unstable for the whole range of power variation of the intermittent source, which in this case is assumed to be within the interval given by [495 605]MW. Notice that the AA based approach is also able to accurately represent unstable cases, with a maximum error of 5% for the simulations considered.

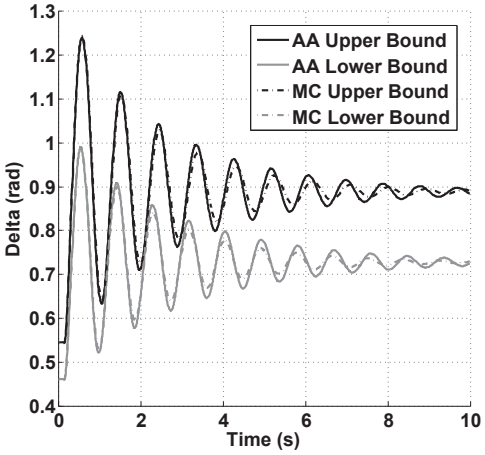

Fig. 6. Generator-Infinite Bus Test System: 3-cycle fault and ±10% variation in generation

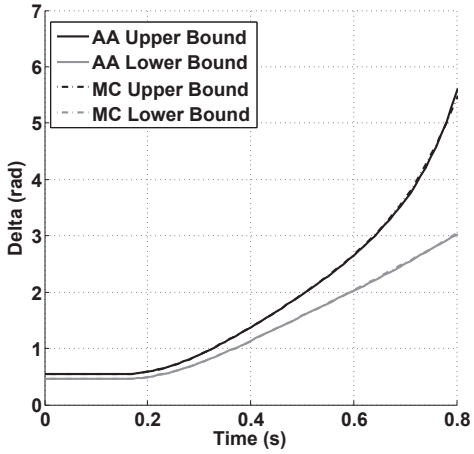

Fig. 7. Generator-Infinite Bus Test System: 33-cycle fault and ±10% variation in generation

Finally, Fig. 8 illustrates the bounds obtained when stable and unstable cases are contained within the assumed interval of power variation of the intermittent source. Thus, observe that the upper bound is unstable, while the lower bound is stable. It is important to point out that in this case, the accuracy of the method for simulation times beyond 0.8 s decreases, due to the significant difference between the curve that bounds unstable cases and the curve that bounds stable cases as time progresses. Nevertheless, for the simulation time considered, the proposed AA based approach is able to identify stable and unstable bounds.

The proposed AA approach was computationally more efficient than MC simulations for all cases, yielding 95.65% (0.798 s vs 18.36 s) savings in computational time for the results depicted in Fig.8.

Conclusions

This paper presented new AA-based paradigms for voltage and transient stability assessment of power systems, considering

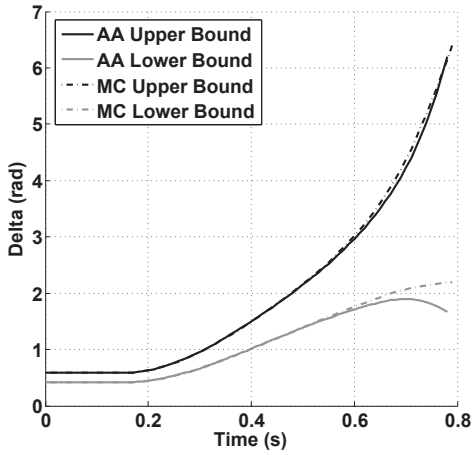

Fig. 8. Generator-Infinite Bus Test System: 30-cycle fault and ±20% variation in generation

uncertainties associated with power injections, which may be attributed to the presence of intermittent sources of power in the system. Both, the proposed AA-based voltage stability method and the AA-based transient stability method were shown to be reasonably accurate and computationally more efficient than typical MC simulations. The accuracy of these AA-based methods can be attributed to their intrinsic characteristic of taking into account the correlations among variables, which is not possible in other self-validated methods such as Interval Arithmetic. The proposed AA-based methods may be used by system operators to evaluate system operation and decide the corrective measures in case of insecure operation for systems with intermittent power sources and/or variable loads.

References

[1] J. Comba and J. Stolfi, "Affine arithmetic and its applications to computer graphics," in *Brazilian Symposium on Computer Graphics and Image Processing VI SIBGRAPI*, 1993, pp. 9–18.

[2] L. de Figueredo and J. Stolfi, "Self-validated numerical methods and applications," in *Brazilian Mathematics Colloq. Monograph IMPA Rio de Janeiro Brazil*, 1997, pp. 1–103.

[3] L. de Figueredo, "Surface intersection using affine arithmetic," in *Graphics Interface'96*, 1996, pp. 168–175.

[4] A. Lemke, L. Hedrich, and E. Barke, "Analog circuit sizing based on formal methods using affine arithmetic," in *IEEE/ACM International Conference on Computer Aided Design, 2002. ICCAD 2002.*, 2002, pp. 486–489.

[5] M. Freisfeld, M. Olbrich, and E. Barke, "Circuit simulations with uncertainties using affine arithmetic and piecewise affine state models," in *9th International Conference on Solid-State and Integrated-Circuit Technology, 2008. ICSICT 2008.*, 2008, pp. 496–499.

[6] A. Vaccaro, C. Cañizares, and D. Villacci, "An affine arithmetic-based methodology for reliable power flow analysis in the presence of data uncertainty," *IEEE Transactions on Power Systems*, vol. 25, no. 2, pp. 624–632, May. 2010.

[7] K. J. Timko, A. Bose, and P. Anderson, "Monte Carlo simulation of power system stability," *IEEE Trans. Power Apparatus and Syst.*, no. 102, pp. 3453–3459, Oct. 1983.

[8] E. Vaahedi, W. Li, T. Chia, and H. Dommel, "Large scale probabilistic transient stability assessment using BC Hydro's on-line tool," *IEEE Trans. Power Syst.*, vol. 15, pp. 661–667, May. 2000.

[9] C. Ferreira, J. Dias Pinto, and F. Barbosa, "Dynamic security analysis of an electric power system using a combined Monte Carlo-hybrid transient stability approach," in *Power Tech Proceedings IEEE Porto*, 2001, pp. 6–12.

[10] W. Wangdee, W. Li, and R. Billinton, "Bulk electric system well-being analysis using sequential Monte Carlo simulation," *IEEE Trans. Power Syst.*, vol. 21, pp. 188–193, Feb. 2006.

[11] A. Leite da Silva, I. Coutinho, A. Zambroni de Souza, R. Prada, and A. Rei, "Voltage collapse risk assessment," *Electr. Power Syst. Res.*, vol. 54, pp. 221–227, Jun. 2000.

[12] A. Rodrigues, R. Prada, and M. Da Guia da Silva, "Voltage stability probabilistic assessment in composite systems: Modeling unsolvability and controllability loss," *IEEE Trans. on Power Syst.*, vol. 25, pp. 1575–1588, Aug. 2010.

[13] S. Chun-Lien and L. Chan-Nan, "Two-point estimate method for quantifying transfer capability uncertainty," *IEEE Transactions on Power Syst.*, vol. 20, no. 2, pp. 573–579, May. 2005.

[14] A. Karimishad and T. Nguyen, "Probabilistic transient stability assessment using two-point estimate method," in *8th International Conference on Advances in Power System Control, Operation and Management (APSCOM 2009)*, 2009, pp. 1–6.

[15] G. Verbic and C. Canizares, "Probabilistic optimal power flow in electricity markets based on a two-point estimate method," *IEEE Transactions on Power Systems*, vol. 21, no. 4, pp. 1883–1893, Nov. 2006.

[16] S. Greene, S. G. Dobson, and F. Alvarado, "Sensitivity of the loading margin to voltage collapse with respect to arbritary parameters," *IEEE Transactions on Power Systems*, vol. 12, no. 1, pp. 262–272, Feb. 1997.

[17] ——, "Sensitivity of transfer capability margins with a fast formula," *IEEE Transactions on Power Systems*, vol. 17, no. 1, pp. 34–40, Feb. 2002.

[18] H. Chen, "Security cost analysis in electricity markets based on voltage security criteria and Web-based implementation," PhD Thesis, University of Waterloo, Waterloo, Canada, 2002.

[19] F. Allella, E. Chiodo, and D. Lauria, "Transient stability probability assessment and statistical estimation," *Electr. Power Syst. Res.*, vol. 67, pp. 21–33, Oct. 2003.

[20] S. Alyasun, Y. Liang, and C. Nwankpa, "A sensitivity approach for computation of the probability density function of critical clearing time and probability of stability in power system transient stability analysis," *Applied Mathematics and Computation*, vol. 176, pp. 563–576, May. 2006.

[21] R. Billinton, P. Kurungaty, and M. Carvalho, "An approximate method for probabilistic assessment of transient stability," *IEEE Trans. Reliability*, vol. 28, pp. 255–258, Aug. 1979.

[22] R. Billinton and P. Kurungaty, "Probabilistic assessment of transient stability in a practical multimachine system," *IEEE Trans. Power Apparatus and Syst.*, vol. 100, pp. 3634–3641, Jul. 1981.

[23] Y. Hsa and C. Chang, "Probabilistic transient stability studies using the conditional probability approach," *IEEE Trans. on Power Syst.*, vol. 3, pp. 1565–1572, Nov. 1988.

[24] R. Billinton and S. Aboreshaid, "Stochastic modelling of high-speed reclosing in probabilistic transient stability studies," in *Generation, Transmission and Distribution*, 1995, pp. 350–354.

[25] D. Z. Fang, L. Jing, and T. Chung, "Corrected Transient Energy Function-based strategy for stability probability assessment of power systems," in *IET Generation, Transmission and Distribution*, 2008, pp. 424–432.

[26] S. O. Faried, R. Billinton, and S. Aboreshaid, "Probabilistic evaluation of transient stability of a power system incorporating wind farms," in *IET Renewable Power Generation*, 2010, pp. 299–307.

[27] H. Kim and C. Singh, "Probabilistic security analysis using SOM and Monte Carlo simulation," in *Power Engineering Society Winter Meeting*, 2002, pp. 755–760.

[28] ——, ""power system probabilistic security assessment using Bayes classifier," *Electr. Power Syst. Res.*, vol. 74, pp. 157–165, Apr. 2005.

[29] A. Dissanayaka, U. Annakkage, B. Jayasekara, and B. Bagen, "Risk-based dynamic security assessment," *IEEE Trans. Power Syst.*, pp. 1–7, Dec. 2010.

[30] B. Jayasekara and U. Annakkage, "Derivation of an accurate polynomial representation of the transient stability boundary," *IEEE Trans. Power Syst.*, vol. 21, no. 3, pp. 1856–1863, Aug. 2006.

[31] L. D. Arya, L. Titare, and D. Kothari, "Determination of probabilistic risk of voltage collapse using Radial Basis Function (RBF) network," *Electr. Power Syst. Res.*, vol. 76, no. 3, pp. 426–434, Apr. 2006.

[32] ——, "Probabilistic assessment and preventive control of voltage security margins using artificial neural network," *International Journal of Electrical Power and Energy Systems*, vol. 29, no. 3, pp. 99–105, Feb. 2007.

[33] B. Leonardi, V. Ajjarapu, M. Djukanovic, and P. Zhang, "Application of multi-linear regression models and machine learning techniques for online voltage stability margin estimation," in *Bulk Power System Dynamics and Control (IREP) - VIII (IREP), 2010 IREP Symposium*, 2010, pp. 1–10.

[34] L. Wang and C. Singh, "Population-based intelligent search in reliability evaluation of generation systems with wind power penetration," *IEEE Transactions on Power Systems*, vol. 23, no. 3, pp. 1336–1345, Aug. 2008.

[35] M. M. Othman, S. Kasim, N. Salim, and I. Musirin, "Risk based uncertainty (RibUt) assessment of a power system using bootstrap technique," in *2012 IEEE International Power Enineering and Optimization Conference (PEDCO) Melaka, Malaysia*, 2012, pp. 460–464.

[36] N. Zhou, J. Pierre, and D. Trudnowski, "A bootstrap method for statistical power system mode estimation and probing signal selection," in *2006 IEEE PES Power Systems Conference and Exposition, 2006. PSCE '06*, 2006, pp. 172–178.

[37] Z. Yang, M. Zwolinski, and C. Chalk, "Bootstrap, an alternative to Monte Carlo simulation," *Electronics Letters*, vol. 34, no. 12, pp. 1174–1175, Jun. 1998.

[38] E. Haesen, C. Bastiaensen, J. Driesen, and R. Belmans, "A probabilistic formulation of load margins in power systems with stochastic generation," *IEEE Transactions on Power Syst.*, vol. 24, no. 2, pp. 951–958, May. 2009.

[39] Y. Kataoka, "A probabilistic nodal loading model and worst case solutions for electric power system voltage stability assessment," *IEEE Transactions on Power Syst.*, vol. 18, no. 4, pp. 1507–1514, Nov. 2003.

[40] S. Senthil Kumar and R. P.Ajay-D-Vimal, "Fuzzy logic based stability index power system voltage stability enhancement," *International Journal of Computer and Electrical Engineering*, vol. 2, no. 1, pp. 24–31, Nov. 2010.

[41] Z. Jing, G. Yun-Feng, and Y. Ming-Hao, "Assessment of voltage stability for real-time operation," in *Power India Conference, 2006 IEEE*, 2006, p. 5.

[42] J. L. Soufis, A. V. Machias, and B. Papadias, "An application of fuzzy concepts to transient stability evaluation of power systems," *IEEE Transactions on Power Syst.*, vol. 4, no. 3, pp. 1003–1009, Aug. 1989.

[43] R. Moore and W. Lodwick, "Interval analysis and fuzzy set theory," *Fuzzy Sets and System*, vol. 135, pp. 5–9, 2003.

[44] R. Albrecht, "Topological theory of fuzziness," in *Int. Conf. Computational Intelligence, Springer, Heidelberg*, 1999, pp. 1–11.

[45] L. Zadeh, "Some reflections on soft computing, granular computing and their roles in the conception, design and utilization of information intelligent systems," *Soft Computing*, vol. 2, pp. 23–25, 1998.

[46] Z. Wang and F. Alvarado, "Interval arithmetic in power flow analysis," *IEEE Trans. Power Systems*, vol. 7, no. 3, pp. 1341–1349, Aug. 1992.

[47] S. Wang, Z. Zheng, and C. Wang, "Power system transient stability simulation under uncertainty based on interval method," in *International Conference on Power System Technology PowerCon*, 2006, pp. 1–6.

[48] D. Grabowski, M. Olbrich, and E. Barke, "Analog circuit simulation using range arithmetics," in *2008 Conf. Asia and South Pacific Design Automation, Seoul, Korea*, 2008, pp. 762–767.

[49] J. Avalos-Muñoz, "Analysis and applications of optmization techniques to power system electricity markets," PhD Thesis, University of Waterloo, Waterloo, Canada, 2008.

[50] J. Mason and D. Handscomb, *Chebyshev polynomials*. Florida, USA: Chapman & Hall/CRC, 2002.

[51] "Voltage stability assessment: Concepts, practices and tools," *IEEE/PES Power System Stability Subcomitte, Tech. Rep.*, Aug. 2002.

[52] T. Van Cutsem and C. Vournas, *Voltage Stability of Electric Power Systems*. New York, USA: Springer, 1998.

[53] V. Ajjarapu and C. Christy, "The continuation power flow: a tool for steady state voltage stability," *IEEE Transactions on Power Systems*, vol. 7, no. 1, pp. 410–423, Feb. 1992.

[54] C. Cañizares and F. L. Alvarado, "Point of collapse and continuation methods for large AC/DC systems," *IEEE Transactions on Power Systems*, vol. 8, no. 1, pp. 1–8, Feb. 1993.

[55] H.-D. Chiang, A. J. Flueck, K. Shah, and N. Balu, "CPFLOW: a practical tool for tracing power system steady-state stationary behavior due to load and generation variations," *IEEE Transactions on Power Systems*, vol. 10, no. 2, pp. 623–634, May. 1995.

[56] J. Duncan-Glover, S. S. Sarma, and T. Overbye, *Power System Analysis and Design*. USA: CENGAGE Learning, 2008.

[57] C. Cañizares, "Angle stability," University Lecture, 2010.